Ruthenic Acid Supercapacitors

Preparation of Ruthenic Acid Nanosheets and Utilization of Its Interlayer Surface for Electrochemical Energy Storage**

Wataru Sugimoto, Hideki Iwata, Yutaka Yasunaga, Yasushi Murakami, and Yoshio Takasu*

Recent advances in materials science have evoked the importance of combining protonics[1–4] and electronics in various applications, such as electrocatalysts for polymer electrolyte fuel cells[5] and electrode materials for electrochemical energy storage.[6–8] This has initiated a challenging search for mixed proton–electron conducting materials containing liquid or liquidlike regions of water to facilitate proton conduction within an electroconducting matrix. The object is to maintain a continuous electroconducting network while incorporating water molecules into the network structure so that the electrolyte can diffuse into the bulk of the electrode material. Crystalline ruthenium oxide is a metallic conductor and is known for its high electrical conductivity, catalytic activity, and excellent chemical, electrochemical, and photochemical stability.[9] It has been used as the main component in commercial Cl_2 evolution electrocatalysts,[10] and has attracted increased interest as bottom-electrode materials,[11] CO oxidizing catalysts,[12,13] and electrode materials for electrochemical supercapacitors.[6–8] Proton conductivity in

[*] Dr. W. Sugimoto, H. Iwata, Y. Yasunaga, Dr. Y. Murakami, Prof. Dr. Y. Takasu
Department of Fine Materials Engineering
Faculty of Textile Science and Technology
Shinshu University, 3-15-1 Tokida, Ueda, Nagano 386-8567 (Japan)
Fax: (+81) 268-22-9048
E-mail: wsugi@giptc.shinshu-u.ac.jp

[**] This work was partially funded by a NEDO Industrial Technology Research Grant Program and a MEXT 21st Century COE Program.

  DOI: 10.1002/ange.200351691

ruthenium-oxide-based materials is an important factor, especially in cases where reactions occur at the solid/liquid interface, as in electrochemical energy devices.[5,6] So far, proton conductivity has been appended to ruthenium-oxide-based materials by the synthesis of hydrous ruthenium oxide with an amorphous structure either by electrochemical oxidation of ruthenium metal or by a sol–gel method. The hydrous structure allows facile proton conduction through the bulk of the material. However, the electrical conductivity of the amorphous phase is slightly lower than in the crystalline phase,[7] which is due to the noncontinuous oxide framework. We recently reported a layered ruthenate that may be a candidate as an electrochemical supercapacitor material.[14] This material consists of an electroconducting crystalline network of ruthenium oxide layers interleaved with a hydrous layer on the nanometer scale.

Here we report the intercalation and exfoliation behavior, and the electrochemical supercapacitor properties of layered ruthenic acid and exfoliated ruthenic acid nanosheets. The layered ruthenic acid is capable of accommodating alkyl ammonium molecules in the interlayer space, and can be exfoliated into individual sheets with lateral dimensions in the order of micrometers and thicknesses in the order of nanometers. This material exhibits a specific capacitance of 658 $F g^{-1}_{(RuO_2)}$, which is a tenfold increase compared to conventional three-dimensional RuO_2,[7,8,14] and comparable to amorphous ruthenium oxide hydrate.[6,7] The high specific capacitance was attributed to the utilization of the interlayer surface for (pseudo)electric double-layer capacitance, which results in an extremely high electrochemical active surface area ($\approx 250\ m^2 g^{-1}$) and utilization of the surface active sites for redox capacitance.

Acid treatment of a potassium ruthenate with a layered structure resulted in a decrease in the basal spacing from 0.7321(1) to 0.457(1) nm (Figure 1). The cation ratio of the products before and after the acid treatment decreased from K/Ru = 0.22:1 to < 0.05:1. Thermoanalysis of the acid-treated product revealed an exothermic reaction between 100–270 °C accompanied by a mass loss of 3 wt %, which can be attributed to dehydroxylation of the interlayer protons. The interlayer proton content based on the mass loss (H/Ru = 0.2:1) is in agreement with the cation ratio of K/Ru = 0.22:1 of the parent potassium ruthenate. These results indicate that the acid treatment of the layered potassium ruthenate yielded a layered ruthenic acid (hereafter designated as HRO) by a topotactic proton-exchange reaction. The composition of HRO based on X-ray photoelectron spectroscopy, inductively-coupled plasma spectroscopy, and thermogravimetry can be expressed as $H_{0.22}RuO_{2.11}\cdot n H_2O$, where n is the interlayer water content and varies with the drying conditions; typically $n \approx 0.9$ for a sample dried at room temperature. The lamellar structure and the crystalline nature of the ruthenium oxide layers was confirmed by electron diffraction (ED) and high-resolution transmission electron microscopy (HRTEM), as shown in Figure 2. The periodicity between the alternating layers of dark and light contrast observed by HRTEM was 0.45 nm, consistent with the basal spacing observed by XRD. The ED patterns of the acid-treated product could be indexed as $a = 0.47$, $b = 0.30$, $c = 0.45$ nm.

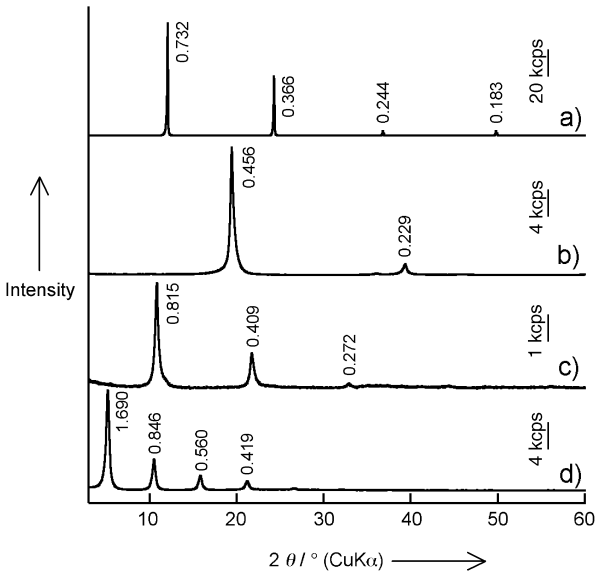

Figure 1. XRD patterns of a) the initial layered potassium ruthenate; b) the product obtained after drying at 120 °C and then undergoing acid treatment; c) the reaction of this product with an aqueous solution of ethylamine; d) the product formed through the subsequent reaction with aqueous tetrabutylammonium hydroxide. The numbers represent the *d* values (units in nm) for each peak.

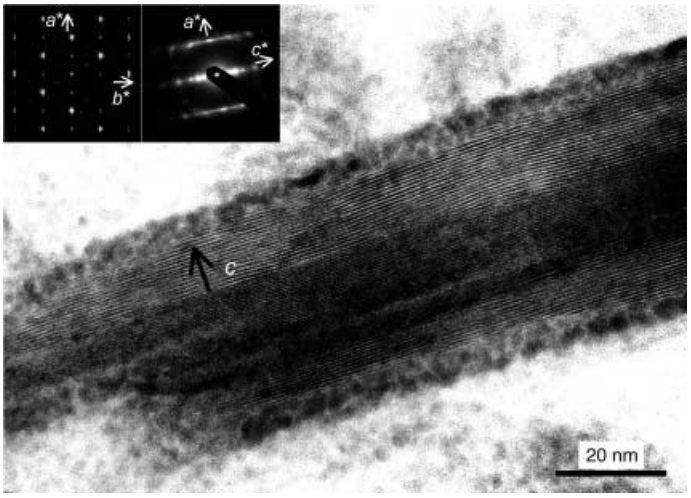

Figure 2. TEM image and ED patterns of layered ruthenic acid.

The lattice parameters suggest that the oxide layer is composed of double-octahedral layers sharing common edges.[15]

Reaction of HRO with aqueous ethylammonium hydroxide resulted in an expansion of the interlayer spacing to 0.816(2) nm, which indicates the formation of an ethylammonium–HRO intercalation compound (Figure 1c). The intercalated ethylammonium ion could be further exchanged with a bulky tetrabutylammonium ion to form a tetrabutylammonium–HRO intercalation compound (basal spacing = 1.68(1) nm) as shown in Figure 1d. The capability of HRO to accommodate alkyl ammonium ions strongly supports the layered structure.

Suspending the tetrabutylammonium–HRO intercalation compound in water resulted in spontaneous exfoliation (delamination) of the ruthenic acid layers into colloidal ruthenic acid nanosheets. After centrifugation at 2000 rpm to separate the relatively large particles and agglomerates, the supernatant-containing exfoliated HRO nanosheets were stable for periods of months with no sedimentation. This stability is due to the weak interaction between the positively charged tetrabutylammonium ions and the negatively charged ruthenium oxide sheets, similar to the exfoliation behavior of layered titanates.[16,17] Figure 3 shows a typical

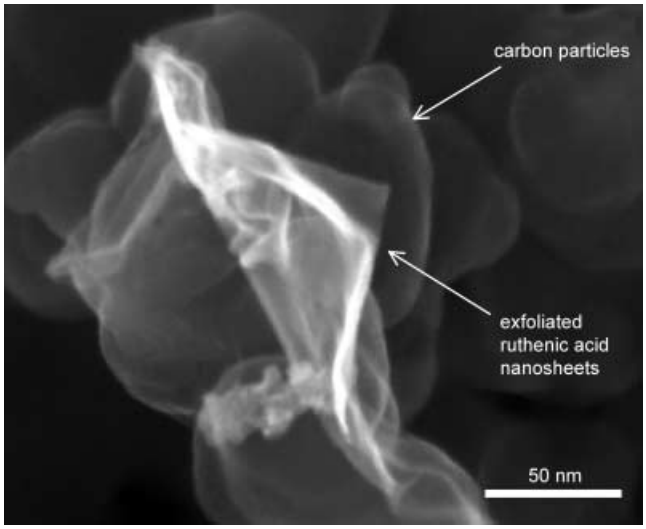

Figure 3. SEM image of exfoliated ruthenic acid nanosheets supported on carbon particles.

scanning electron micrograph of the exfoliated HRO nanosheets supported on carbon particles, which reveal platelike sheets with lateral dimensions in the range of micrometers and thicknesses in the order of nanometers. The exfoliated HRO nanosheets can be reassembled into a *c*-axis-oriented thin film of the tetrabutylammonium–ruthenic acid intercalation compound by casting the material onto a flat substrate.

Cyclic voltammagrams of pristine (non-exfoliated) HRO recorded at sweep rates between 2 and 500 $mV\,s^{-1}$ are shown in Figure 4. The square-shaped "background" of the CV (shaded region) is characteristic of (pseudo)electric double-layer capacitance (outer- and inner-Helmholtz plane charging) and is independent of the sweep rate. In addition to the (pseudo)electric double-layer capacitance, multiple redox peaks characteristic of surface redox reactions can be observed. Such redox peaks are typical features of crystalline RuO_2, and are not observed in amorphous ruthenium oxide hydrate. The specific capacitance at 2 $mV\,s^{-1}$ was 392 $F\,g^{-1}_{(RuO_2)}$. Even at a fast sweep rate of 500 $mV\,s^{-1}$, the specific capacitance was 329 $F\,g^{-1}_{(RuO_2)}$, which is representative of excellent fast charge/discharge properties (Figure 4). These results indicate that HRO is a mixed proton–electron conductor, in which the ruthenate layers contribute to the electrical conductivity and the hydrated interlayer allows

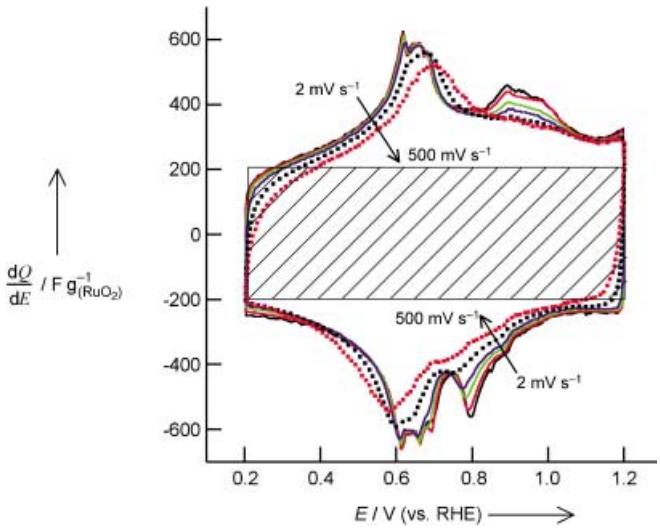

Figure 4. Steady-state cyclic voltammograms of layered ruthenic acid hydrate in 0.5 M H_2SO_4 (25 °C) at scan rates of 2 to 500 $mV\,s^{-1}$. The contribution from the (pseudo)electric double-layer capacitance is shown in the shaded region (dQ/dE = differential capacitance).

diffusion of the electrolyte (proton conductivity) into the bulk of the material.

The (pseudo)electric double-layer capacitance (shaded region in Figure 4) was independent of the sweep rate at approximately 200 $F\,g^{-1}_{(RuO_2)}$. By using a surface charge density of 80 $\mu C\,cm^{-2}$ as a measure for evaluation of the electrochemically active surface area,[18] this specific capacitance value gives an electrochemically active surface area of 250 $m^2\,g^{-1}$. This is much higher than the BET surface area of 57 $m^2\,g^{-1}$ determined by N_2 adsorption/desorption measurements. The difference is attributed to the fact that the BET surface area is a measurement of the outer surface area of anhydrous HRO, and does not include the hydrated interlayer surface area. Using the density of rutile-type RuO_2 ($\approx$7.1 $g\,cm^{-3}$), a specific surface area of 250 $m^2\,g^{-1}$ will yield a rectangular particle with a thickness of $\approx$0.6 nm, in good agreement with the observed thickness of ruthenic acid layers. The remarkably high specific capacitance can only be explained by assuming that the interlayer surface is utilizable for electrochemical charge storage. As shown in Figure 5 the capacitance loss after 10000 consecutive cycles was negligible, a fact that reveals the excellent electrochemical stability of HRO.

Cyclic voltammograms of the exfoliated HRO nanosheets are shown in Figure 6. The general electrochemical behavior of the exfoliated HRO nanosheets is comparable to that of the pristine HRO. However, the redox peaks are more well-defined for the exfoliated HRO nanosheets; that is, the contribution from the redox capacitance is more pronounced for the exfoliated nanosheets. This results in a significantly higher specific capacitance (658 and 601 $F\,g^{-1}_{(RuO_2)}$ at 2 and 50 $mV\,s^{-1}$, respectively) as shown in Figure 7. The (pseudo)-electric double-layer capacitance for both pristine HRO and exfoliated HRO nanosheets is $\approx$200 $F\,g^{-1}_{(RuO_2)}$, which illustrates that the electrochemically active surface area is the same (250 $m^2\,g^{-1}$) for both systems. The increase in the surface

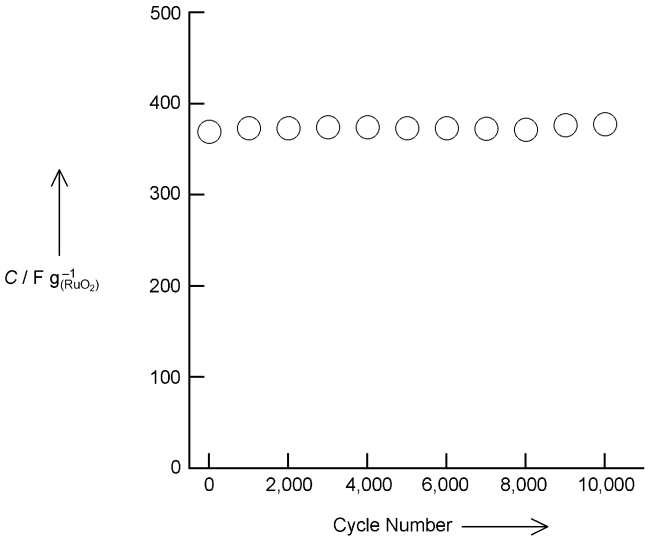

Figure 5. The specific capacitance of layered ruthenic acid hydrate in 0.5 M H_2SO_4 (25 °C) at scan rates of 50 mV s^{-1} as a function of the cycle number (C = specific capacitance).

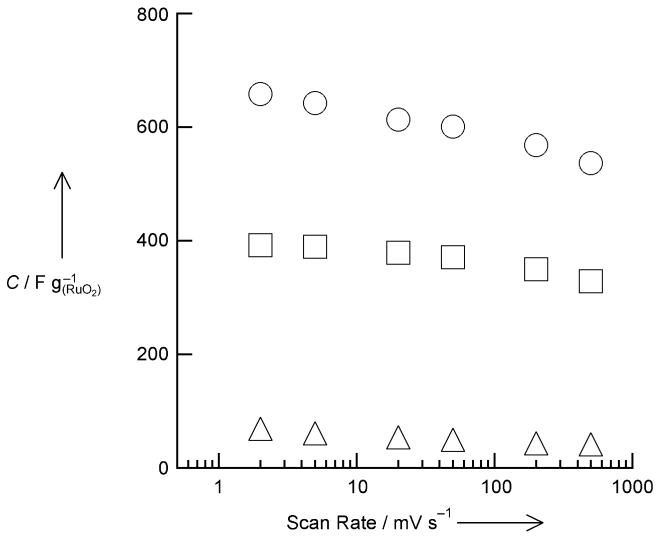

Figure 7. The specific capacitance as a function of the scan rate for rutile-type RuO_2 (△), layered ruthenic acid (□), and exfoliated ruthenic acid nanosheets (○) in 0.5 M H_2SO_4 at 25 °C.

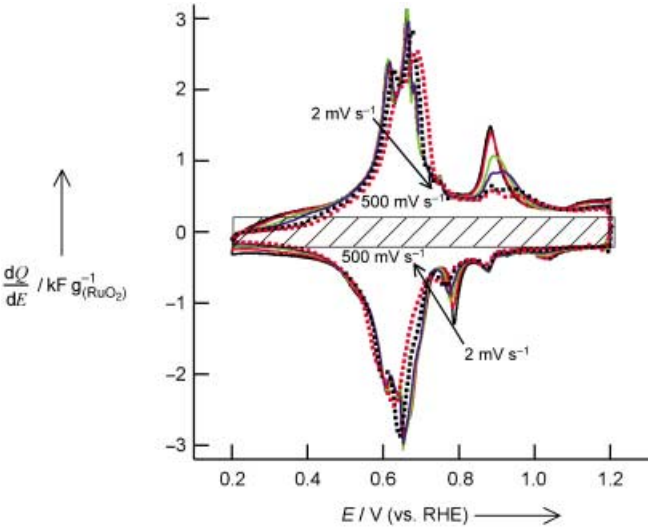

Figure 6. Steady-state cyclic voltammograms of exfoliated ruthenic acid nanosheets in 0.5 M H_2SO_4 (25 °C) at scan rates of 2 to 500 mV s^{-1}. The contribution from the (pseudo)electric double-layer capacitance is shown in the shaded region.

redox capacitance may be due to an increase in diffusion-limited capacitance owing to the more open framework of the exfoliated ruthenium oxide nanosheets compared to pristine HRO. The specific capacitance of the exfoliated HRO nanosheets is 10 times higher than nanocrystalline rutile-type RuO_2 (68 F g$^{-1}_{(RuO_2)}$ at 2 mV s^{-1}) with a similar BET surface area (52 m^2 g^{-1}).[19,20] The specific capacitance is comparable to that of sol–gel-derived or commercial amorphous ruthenium oxide hydrate (≈700 F g^{-1} at 2 mV s^{-1}).[6,7] The specific capacitance of HRO, exfoliated HRO nanosheets, and rutile-type RuO_2 decreases only slightly with increasing scan rate, as shown in Figure 7. The decreasing ratio is similar for the three systems, that is approximately 60–80% of the capacitance addressable at a scan rate of 2 mV s^{-1} can be achieved at 500 mV s^{-1}. Such observations indicate that the iR loss (voltage drop) due to inter- and inner-particle resistance of HRO is similar to rutile-type RuO_2. Thus it can be presumed that the electronic conductivity of HRO is similar to rutile-type RuO_2, and the electrochemical accessibility of the interlayer of HRO is comparable to the surface of rutile-type RuO_2.

In conclusion, we have demonstrated the synthesis of a mixed proton–electron conductor consisting of a crystalline ruthenium oxide layer interleaved with layers of water (Figure 8). The layered ruthenic acid is electrochemically stable, and has an extremely large electrochemically active surface area. The layered ruthenic acid has an expandable interlayer and can be delaminated into colloidal ruthenic acid nanosheets. The present material is a promising electrode material for electrochemical supercapacitors that can provide high energy density even at high-power specifications. From

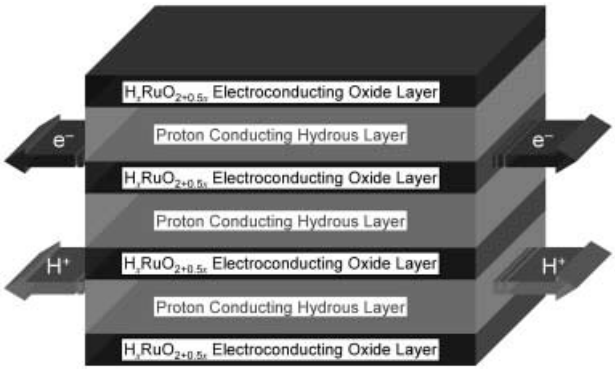

Figure 8. A schematic drawing of the concept of the mixed proton–electron conductivity of layered ruthenic acid.

the viewpoint of materials chemistry, the present results should unearth a new class of mixed proton–electron conductors. The new layered ruthenium oxide hydrate adds a new dimension to the rapidly growing toolbox of layered compounds for novel soft-chemistry reactions.[21,22] The use of crystalline layered oxides will permit synthetic conditions that will furnish compositional and structural variety by traditional ceramic processing methods. Based on existing materials, one can postulate that partial substitution of Ru with transition metals such as Ti, V, Ir, etc. in the crystalline structure can be accomplished. Furthermore, the versatility of the oxide sheets to exfoliate into multilamellar to unilamellar nanosheets allows further flexibility for morphological control (thin films, "house-of-cards" structures, exfoliated nanosheets, etc.).[22,23]

Experimental Section

The layered potassium ruthenate was synthesized by calcination of a pelletized mixture of K_2CO_3 and RuO_2 (5:8 molar ratio) at 850 °C for 12 h under a flow of Ar. The product was ground into a fine powder then washed with copious amounts of water and dried at 120 °C. The layered ruthenic acid was prepared by acid treatment of the potassium ruthenate at 60 °C for 48 h, followed by washing with copious amounts of water and drying at 120 °C.

An ethylammonium-layered ruthenic acid intercalation compound was prepared by reaction of the layered ruthenic acid with an aqueous solution (50 %) of ethylamine at room temperature for 24 h. The solid product was centrifugally collected (15000 rpm), washed with acetone, and vacuum dried. A tetrabutylammonium-layered ruthenic acid intercalation compound was prepared by reaction of the ethylammonium–ruthenic acid intercalation compound with an aqueous solution (10 %) of tetrabutylammonium hydroxide at room temperature for 50 h. The solid product was centrifugally collected (15000 rpm). The solid product (the tetrabutylammonium-layered ruthenic acid intercalation compound) was then dispersed in distilled water and subjected to ultrasonification for 15 min. The supernatant containing exfoliated HRO nanosheets and other relatively large particles and agglomerates were centrifugally separated at 2000 rpm. The supernatant was then used for further investigation.

Electrochemical measurements were conducted in 0.5 M H_2SO_4 at 25 °C with a half-cell set up. A beaker-type electrochemical cell equipped with the working electrode, a platinum mesh counter electrode, and a Ag/AgCl reference electrode was used for electrochemical measurements. A Luggin capillary faced the working electrode at a distance of 2 mm. The working electrode was prepared by the thin-film electrode method.[24] For the characterization of pristine (non-exfoliated) HRO particles, HRO (20 mg) was dispersed in distilled water (10 mL) and then subjected to ultrasonification for 30 min. Then, while stirring, 20 μL of the HRO dispersion was extracted using a micropipette and dropped onto a mirror-polished glassy carbon rod (5-mm diameter). After drying the HRO-modified glassy carbon rod at 60 °C, 20 μL of a 1 wt % nafion ionomer solution was dropped onto the rod and dried at 60 °C to affix the active material onto the glassy carbon surface. For the exfoliated HRO nanosheets, 20 μL was extracted from a 1:10 diluted supernatant containing exfoliated HRO nanosheets (1.8 mg of RuO_2 per 10 mL of distilled water) and dropped onto a mirror-polished glassy carbon rod. The tetrabutylammonium intercalant should exchange with protons (deintercalate) in the acidic electrolyte. Cyclic voltammetry was conducted in a 0.5 M H_2SO_4 electrolyte with scan rates between 2 and 500 mV s^{-1} at 25 °C. The voltammagrams were recorded after 500 break-in cycles at 50 mV s^{-1}. The specific capacitance was determined by integration of the enclosed area of the anodic and cathodic curves in the cyclic voltammagrams between 0.20–1.20 V (versus a reversible hydrogen electrode (RHE)). The average of the anodic and cathodic charges was used to calculate the specific capacitance, which are reported in units of farads per unit mass of RuO_2 ($F g^{-1}_{(RuO_2)}$) to allow uncomplicated comparison between different systems.

Received: April 17, 2003 [Z51691]

Keywords: electrochemistry · intercalations · layered compounds · mixed conductors · supercapacitors

[1] H. Iwahara, *Proceedings 17th Risø International Symposium of Material Science* (Eds.: F. W. Poulsen, N. Bonanos, S. Linderoth, M. Mogenson, B. Zachau-Christiansen), Risø National Laboratories, Roskilde, Denmark, **1996**, p. 13.
[2] H. L. Tuller, *J. Phys. Chem. Solids* **1994**, *55*, 1393.
[3] K. D. Kreuer, *Chem. Mater.* **1996**, *8*, 610.
[4] Ph. Colomban, *Proton Conductors*, Cambridge Universitry Press, Cambridge, **1992**.
[5] J. W. Long, R. M. Stroud, K. E. Swider-Lyons, D. R. Rolison, *J. Phys. Chem. B* **2000**, *104*, 9772.
[6] J. P. Zheng, T. R. Jow, *J. Electrochem. Soc.* **1995**, *142*, L6.
[7] J. P. Zheng, P. J. Cygan, T. R. Jow, *J. Electrochem. Soc.* **1995**, *142*, 2699.
[8] B. Conway, *Electrochemical Supercapacitors*, Kluwer Academic/Plenum Publishers, New York, **1999**.
[9] S. Trasatti in *Electrodes of Conducting Metal Oxides*, (Ed.: S. Trasatti), Elsevier, Amsterdam, **1980**, p. 301 – 358.
[10] S. Trasatti, *Electrochim. Acta* **1991**, *36*, 225.
[11] R. Dat, D. J. Lichtenwalner, O. Auciello, A. I. Kingon, *Appl. Phys. Lett.* **1994**, *64*, 2673.
[12] H. Over, Y. D. Kim, A. P. Seitsonen, S. Wendt, Lundgren, M. Schmid, P. Varga, A. Morgante, G. Ertl, *Science* **2000**, *287*, 1474.
[13] L. Zang, H. Kisch, *Angew. Chem.* **2000**, *112*, 4075; *Angew. Chem. Int. Ed.* **2000**, *39*, 3921.
[14] Y. Takasu, Y. Murakami, *Electrochim. Acta* **2000**, *45*, 4135.
[15] B. Raveau, *Rev. Inorg. Chem.* **1987**, *9*, 37.
[16] T. Sasaki, M. Watanabe, H. Hashizume, H. Yamada, H. Nakazawa, *J. Am. Chem. Soc.* **1996**, *118*, 8329.
[17] W. Sugimoto, O. Terabayashi, Y. Murakami, Y. Takasu, *J. Mater. Chem.* **2002**, *12*, 3814.
[18] P. Siviglia, A. Daghetti, S. Trasatti, *Colloids Surf.* **1983**, *7*, 15.
[19] W. Sugimoto, T. Shibutani, Y. Murakami, Y. Takasu, *Electrochem. Solid-State Lett.* **2002**, *5*, A170.
[20] W. Sugimoto, T. Kizaki, K. Yokoshima, Y. Murakami, Y. Takasu, unpublished results.
[21] W. Sugimoto, M. Shirata, Y. Sugahara, K. Kuroda, *J. Am. Chem. Soc.* **1999**, *121*, 11601.
[22] R. E. Schaak, T. E. Mallouk, *Chem. Mater.* **2002**, *14*, 1455.
[23] C. N. R. Rao, J. Gopalakrishnan, *New Directions in Solid State Chemistry*, 2nd ed., Cambridge University Press, Cambridge, **1997**.
[24] T. J. Schmidt, H. A. Gasteiger, G. D. Stäb, P. M. Urban, D. M. Kolb, R. J. Behm, *J. Electrochem. Soc.* **1998**, *145*, 2354.

